

Numerical Simulation and Experimental Study on Process of Icing and Metal Surface Separation

WANG Shaolong^{1,2,4*}, JI Yanzhuo^{3,4}, KANG Yuhao^{3,4}, SHI Lei^{3,4}, ZHANG Liang^{3,4}

1. School of Metallurgy and Energy, North China University of Science and Technology, Tangshan 063210, P. R. China; 2. Key Laboratory of Icing and Anti/De-icing, China Aerodynamics Research and Development Center, Mianyang 621000, P. R. China; 3. College of Mechanical and Electrical Engineering, Hebei Normal University of Science and Technology, Qinhuangdao 066000, P. R. China; 4. Hebei Technology Innovation Center of Photovoltaic Module Manufacturing Equipment, Hebei Normal University of Science and Technology, Qinhuangdao 066000, P. R. China

(Received 18 March 2023; revised 20 August 2023; accepted 5 September 2023)

Abstract: It is of great significance to optimize de-icing methods by studying the adhesion characteristics between icing and object surfaces, as well as mastering the separation process between them. Although nano-scale numerical simulations provide some insights into the icing separation process, they fail to fully capture the complexities of real-world icing phenomena. Hence, there is a need to investigate the macro-scale icing separation process. We have constructed a test bench capable of assessing icing adhesion in both the normal and tangential directions. By conducting experiments at different temperatures, we have obtained valuable data on the change in normal and tangential adhesion between icing icicles and metal surfaces. Moreover, we have introduced a macroscopic icing adhesion model and incorporated a constitutive model for the cohesion unit layer. This facilitates the numerical simulation of the separation process between icing and metal surfaces in Abaqus software. By validating simulation results with experimental data, we gain insights into the characteristics of icing adhesion and achieve a better understanding of the icing and metal sheet separation process.

Key words: ice; adhesion; separation process; metal surface; numerical simulation

CLC number: TB306

Document code: A

Article ID: 1005-1120(2023)S1-0042-08

0 Introduction

Formation and accretion of ice can hinder the operation of critical systems in the national infrastructure, such as aircraft^[1], power lines^[2], wind turbines^[3], ships^[4] and telecommunications equipment. The removal of ice is necessary to prevent dangerous situations and unwanted icing in our daily lives. Ice can be dislodged when an external force exceeds the adhesion between the ice and the surface. Current de-icing methods primarily focus on increasing the external force applied to the ice, such as by tapping or vibrating the ice. Another approach is to reduce the adhesion between the ice and the object surface, which can be achieved through

the use of ice-thinning coatings or heating methods. It is of great importance to optimize de-icing methods by studying the adhesion characteristics between ice and object surfaces and understanding the separation process between them^[5-6].

There are two main ways to study the separation characteristics of icing and objects. One is to build an icing adhesion characteristics test device to directly carry out the test^[7-9], which provides an intuitive and accurate reflection of the actual process of icing and surface separation. However, it is often limited by experimental conditions. The other approach is to simulate the icing and object separation process numerically, which is not constrained by ic-

*Corresponding author, E-mail address: wangsl@ncst.edu.cn.

How to cite this article: WANG Shaolong, JI Yanzhuo, KANG Yuhao, et al. Numerical simulation and experimental study on process of icing and metal surface separation[J]. Transactions of Nanjing University of Aeronautics and Astronautics, 2023, 40(S1):42-49.

<http://dx.doi.org/10.16356/j.1005-1120.2023.S1.004>

ing experimental conditions and allows for simulation under various working conditions. In one study, atomistic modeling and molecular dynamics simulations were used to investigate the correlation between water contact angle and ice adhesion^[10]. Nano-scale numerical simulations of the ice adhesion are attractive because they eliminate many variables that affect macro-scale ice failure. Nonetheless, determining the true contact area in such simulations is very challenging, and they may not necessarily relate to practical ice removal scenarios. Therefore, macro-scale ice adhesion measurement methods will be discussed in the following sections.

In this study, we initially established an icing adhesion test bench to obtain the macroscopic bonding characteristics between icing and metal surfaces. By analyzing the tangential and normal bonding characteristics, we determined the macroscopic bonding mechanism between icing and metal surfaces. Subsequently, we constructed a cohesive constitutive model between ice and the thickness. Finally, we performed numerical simulations of the icing and metal surface separation process using Abaqus numerical simulation software.

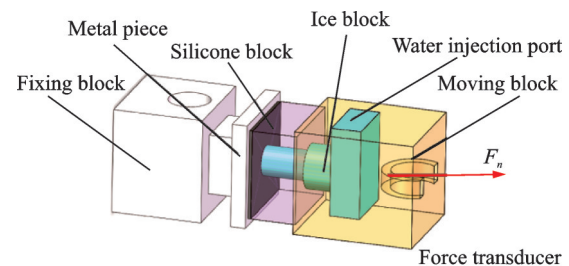
1 Measurement of Icing Adhesion on Metal Surface

1.1 Adhesion test system

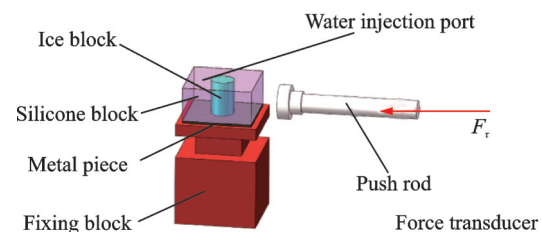
We have designed an experimental system to test the normal adhesion and tangential adhesion between icing and metal surfaces, as illustrated in Fig.1. A 1 mm thick Q235 cold-rolled steel plate was selected and treated without modification to accurately represent real icing conditions. The test specimens were selected with dimensions of 30 mm × 30 mm. Prior to each experiment, the surface roughness of the randomly chosen iron sheets was measured using a roughness measuring instrument (JITA1820), resulting in a range of 0.15—0.25 μm. To ensure the cleanliness of the iron sheet, its surface was placed in alcohol, and then cleaned with ultrasonic waves for 10 min. The vertical adhesion test fixture is depicted in Fig.1(a), where the metal piece and the fixing block are securely fastened us-

ing bolts. A silicone block is attached to the metal sheet, and a moving block is then connected to the silicone block. The entire setup is filled with pure water through the water injection port and placed in a refrigerator. Once the pure water freezes and forms an ice block, it becomes bonded to the metal sheet. By pulling the moving block to separate the ice block from the metal sheet, we can obtain the vertical bonding force F_n between the ice block and the metal piece. The shear adhesion test fixture is shown in Fig.1(b), where the metal sheet and the fixing block are also fastened together using bolts. A silicone block is attached to the metal sheet. Similar to the vertical adhesion test, pure water is filled through the water injection port and the setup is placed in a refrigerator to freeze the water into an ice block. By pulling the ice block, we can determine the shear bonding force F_t between the ice block and the metal piece.

During the testing process, the force measuring device is operated in a low-temperature test environment. The entire device is placed inside a low-



(a) Vertical adhesion test fixture



(b) Shear adhesion test fixture

Fig.1 Adhesion test fixture

temperature test box, as illustrated in Fig.2. To ensure accurate temperature measurements, the device is cooled within the low-temperature experiment box for a minimum of 1 h. This allows the ice and metal sheet to reach the desired temperature before initiating the testing procedure. Once the desired temperature is achieved, the drive motor is activated to commence the testing process.

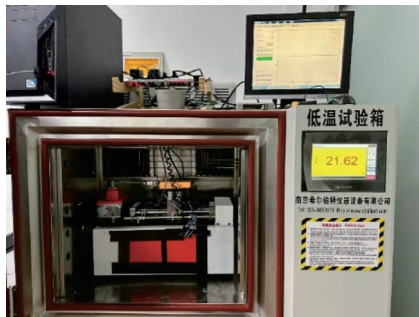


Fig.2 Low-temperature test device

1.2 Adhesion test results

The adhesion tests were conducted under the conditions outlined in Table 1. Each working condition was repeated four times, and the average of the multiple test results was calculated for subsequent analysis.

Table 1 Test conditions

Working condition	Ice column diameter d/mm	Ambient temperature $T/^\circ\text{C}$	Force measurement method
Case 1	10	-12	Vertical
Case 2	10	-10	Vertical
Case 3	10	-8	Vertical
Case 4	10	-6	Vertical
Case 5	10	-4	Vertical
Case 6	10	-3	Vertical
Case 7	10	-2	Vertical
Case 8	10	-12	Shear
Case 9	10	-10	Shear
Case 10	10	-8	Shear
Case 11	10	-6	Shear
Case 12	10	-4	Shear
Case 13	10	-3	Shear
Case 14	10	-2	Shear

Fig.3 presents the test results for the adhesion forces (F) and adhesion stress (σ) under different working conditions. Fig.3 demonstrates that as the

temperature decreases, both the vertical adhesion and shear adhesion forces exhibit an increasing trend. Between temperatures ranging from -4°C to -8°C , the vertical and shear adhesion forces remain relatively steady. However, beyond -4°C , both forces decrease rapidly, while they increase rapidly when the temperature exceeds -8°C . It can be observed that under identical working conditions, the values of the vertical adhesion force and shear adhesion force are similar.

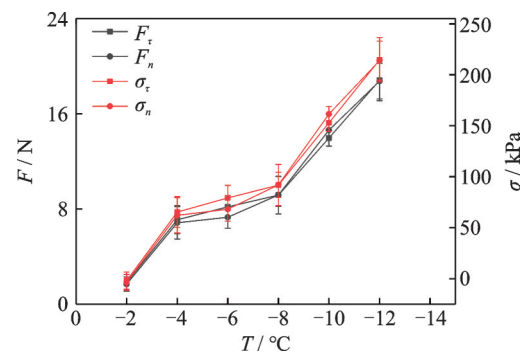


Fig.3 Adhesion test results

2 Adhesion Mechanism Between Icing and Metal Piece

2.1 Ice separation mechanism

Currently, there is no universally accepted theory that explains the mechanism of freezing adhesion between icing and a solid wall. It is generally acknowledged that the adhesion force is a combination of chemical bond forces, intermolecular forces, and mechanical forces. The main factors influencing adhesion are the material properties of the solid wall, such as material type, roughness, and hydrophobic properties, as well as the composition of the frozen water, freezing method, and ambient temperature.

Under identical conditions, the bond strength between the ice and the solid wall tends to remain constant, with slight fluctuations due to the inherent randomness of ice. When the ice is separated from a flat plate, the adhesion force F generated along the separation direction can be divided into normal cohesive force F_n and tangential cohesive force F_t , as depicted in Fig.4. The separation adhesion stress τ sat-

isfies Eq.(1) and can be further decomposed into vertical adhesion stress τ_n and shear adhesion stress τ_τ , which are governed by Eqs.(2, 3), respectively. Here, A_{ice} represents the contact area between the ice and the surface. During the analysis of the separation process between icing and the surface, the focus lies in the relationship between icing and the surface of the object. To capture the adhesive characteristics of icing, a adhesive unit layer is introduced on the surfaces of both the icing and the solid. The failure mode of the adhesive unit layer reflects the adhesion characteristics of icing.

$$\tau = F/A_{ice} \quad (1)$$

$$\tau_n = F_n/A_{ice} \quad (2)$$

$$\tau_\tau = F_\tau/A_{ice} \quad (3)$$

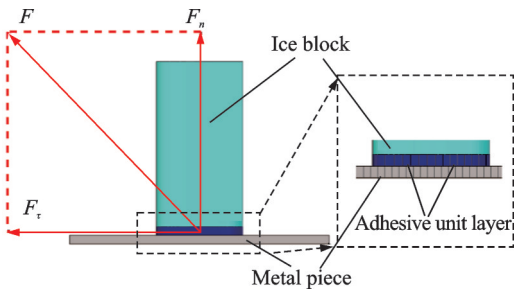


Fig.4 Adhesion force model

2.2 Model of adhesion force

The adhesive force model method is a numerical simulation approach used to analyze the separation process between two bonded substances^[11]. It is founded on the principles of damage mechanics and the description of crack propagation. This method combines the strengths of both finite element and discrete element algorithms. By utilizing the adhesive force model, the finite element method facilitates the analysis of continuous mechanical problems, while the discrete element method is beneficial to the analysis of mechanical problems involving large deformations. This integration allows for a more comprehensive simulation of the separation process.

This article employs a bilinear adhesive force model, and its constitutive relationship is depicted in Fig.5. The OA line segment in the figure represents the linear elastic stage of the adhesive unit.

The A point signifies the initiation of adhesive unit damage, while the AB line segment represents the progression of adhesive unit damage. The nominal peak stress is represented by points t_n^0 , t_s^0 , and t_l^0 , corresponding to complete deformation perpendicular to the cohesive unit separation interface or entirely in the first or second shear direction. The corresponding interface separation displacements are denoted as δ_n^0 , δ_s^0 and δ_l^0 . Furthermore, the separation displacements and critical fracture energies of the failure interface in the three directions are represented by δ_n^f , δ_s^f , δ_l^f and G_n^c , G_s^c , G_l^c , respectively.

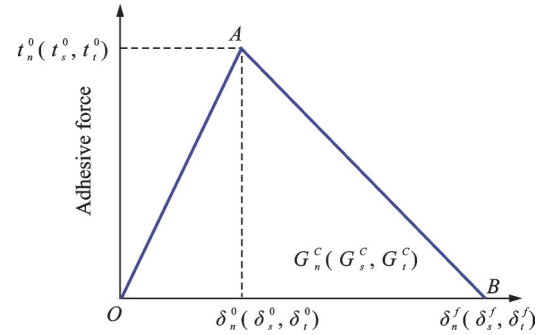


Fig.5 Adhesive force model

The nominal traction stress vector \mathbf{t} consists of three components representing the stress in three directions: t_n , t_s and t_l . The corresponding separation quantities are denoted as δ_n , δ_s and δ_l . The variable T_0 represents the initial thickness of the adhesive element. The nominal strain can be expressed as

$$\epsilon_n = \delta_n/T_0 \quad (4)$$

$$\epsilon_s = \delta_s/T_0 \quad (5)$$

$$\epsilon_l = \delta_l/T_0 \quad (6)$$

The elastic behavior of the adhesive unit is described by Eq.(7). To determine if the cohesive element has reached the damage initiation point, the maximum nominal stress criterion shown in Eq.(8) can be utilized.

$$\mathbf{t} = \begin{bmatrix} t_n \\ t_s \\ t_l \end{bmatrix} = \begin{bmatrix} E_{nn} & & \\ & E_{ss} & \\ & & E_{ll} \end{bmatrix} \begin{Bmatrix} \epsilon_n \\ \epsilon_s \\ \epsilon_l \end{Bmatrix} = \mathbf{E}_\epsilon \quad (7)$$

$$\max \left\{ \frac{\langle t_n \rangle}{t_n^0}, \frac{t_s}{t_s^0}, \frac{t_l}{t_l^0} \right\} = 1 \quad (8)$$

$$\langle t_n \rangle = \begin{cases} t_n & t_n > 0 \\ 0 & t_n \leq 0 \end{cases} \quad (9)$$

The damage evolution law describes the rate at which the stiffness of the cohesive unit degrades after reaching the damage initiation point, as shown in

$$t_n = \begin{cases} (1-D)\bar{t}_n & \bar{t}_n > 0 \\ \bar{t}_n & \bar{t}_n \leq 0 \end{cases} \quad (10)$$

$$t_s = (1-D)\bar{t}_s \quad (11)$$

$$t_t = (1-D)\bar{t}_t \quad (12)$$

where \bar{t}_n , \bar{t}_s and \bar{t}_t represent the stress components of the current undamaged strain predicted by the cohesive unit's traction-separation constitutive model; D is the stiffness degradation coefficient, $D \in [0, 1]$.

G_n , G_s , and G_t are used to represent the work conducted by the traction force in the normal, the first, and the second tangential directions, respectively. $G_T = G_n + G_s + G_t$ and $G_S = G_s + G_t$ are defined to represent the work conducted by two tangential gravitational components. The area under the traction separation curve is equal to the fracture energy, and the damage evolution law under mixed mode adopts the Benzeggagh-Kenane cracking criterion^[12], and is described as

$$G_n^c + (G_s^c - G_n^c) \left\{ \frac{G_s}{G_T} \right\}^\eta = G^c \quad (13)$$

where $G_s^c = G_t^c$, G^c is the mixed mode fracture energy; η the material parameter.

3 Numerical Simulation of Icing Separation Process

This paper aims to validate and compare the experimental results with the simulation results. The good agreement between them will confirm the feasibility of using Abaqus to simulate the ice and metal plane separation process. For the modeling process, an adhesive model was adopted, involving two components: The metal flat plate and the ice block. The metal flat plate was modeled using eight-node solid elements of type C3D8R, with dimensions of 30 mm × 30 mm × 1 mm. Similarly, the ice block was modeled using eight-node solid elements of type C3D8R, with dimensions of $\varnothing 10$ mm × 20 mm. In the mesh generation, careful consideration was given to the balance between the density of the mesh with the impact on calculation results, compu-

tational workload, and time. The metal flat plate component was assigned a mesh size of 0.5 mm. The icing component's mesh size was 0.5 mm, and the cohesive unit's mesh size 0.5 mm. The resulting mesh division is illustrated in Fig.6.

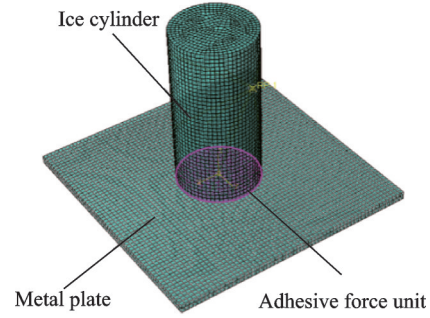


Fig.6 Mesh division

The adhesive force model ensures the generality of crack initiation and propagation during the separation process of metal plates and ice by incorporating adhesive force elements at the shared interface between the metal plates and ice blocks. By obtaining the finite element node information of the interface, a cohesive element is introduced in the interaction module to create the interface effectively and efficiently.

The model utilizes specific material parameters for each component, as presented in Table 2. For the separation process, brittle materials are employed for the ice blocks, while rigid materials are used for the metal plates. The interface between them adopts a cohesive force model, where the bonding strength σ_{\max} is defined based on the values obtained from Fig.3 under different temperature conditions. Similarly, the corresponding normal phase and tangential first fracture energy values are set according to the conditions depicted in Fig.3. The loading method employed in the simulation is displacement loading, and the loading step involves static analysis. The metal flat component is fixed in its position, while the ice block component is subjected to movement along the normal and tangential directions at a velocity of 0.001 m/s until separation occurs between the frozen component and the metal component. Throughout this process, the adhesive force between the frozen component and the metal flat component is continuously monitored.

Table 2 Material parameters

Parameter	Ice cylinder	Metal plate
Density/(kg·m ³)	920	7 850
Elastic modulus/MPa	800	2E11
Poisson's ratio	0.28	0.3

Reproduce the process of icing and metal separation through numerical simulation. The maximum adhesion force generated during this separation process is selected and analyzed as the actual adhesion force. By considering the working conditions outlined in Table 1, the simulation results are compared with corresponding test results, as shown in Fig.7. Observations from this comparison show there is a close match between the calculated limit value of linear separation and the adhesion force obtained in the test. This successful agreement highlights the capability of Abaqus in effectively simulating and numerically analyzing the separation processes between icing and metal plates.

Fig.8 displays the stress variation cloud diagram during the separation process between the ice column and the iron sheet under case 1 and case 8 conditions, where Fig.8(a) shows the variation of stress cloud map with time under case 1 and Fig.8(b) shows the variation of stress cloud map with time under case 8. It reveals that with the

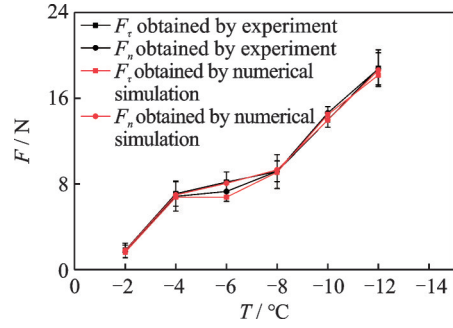


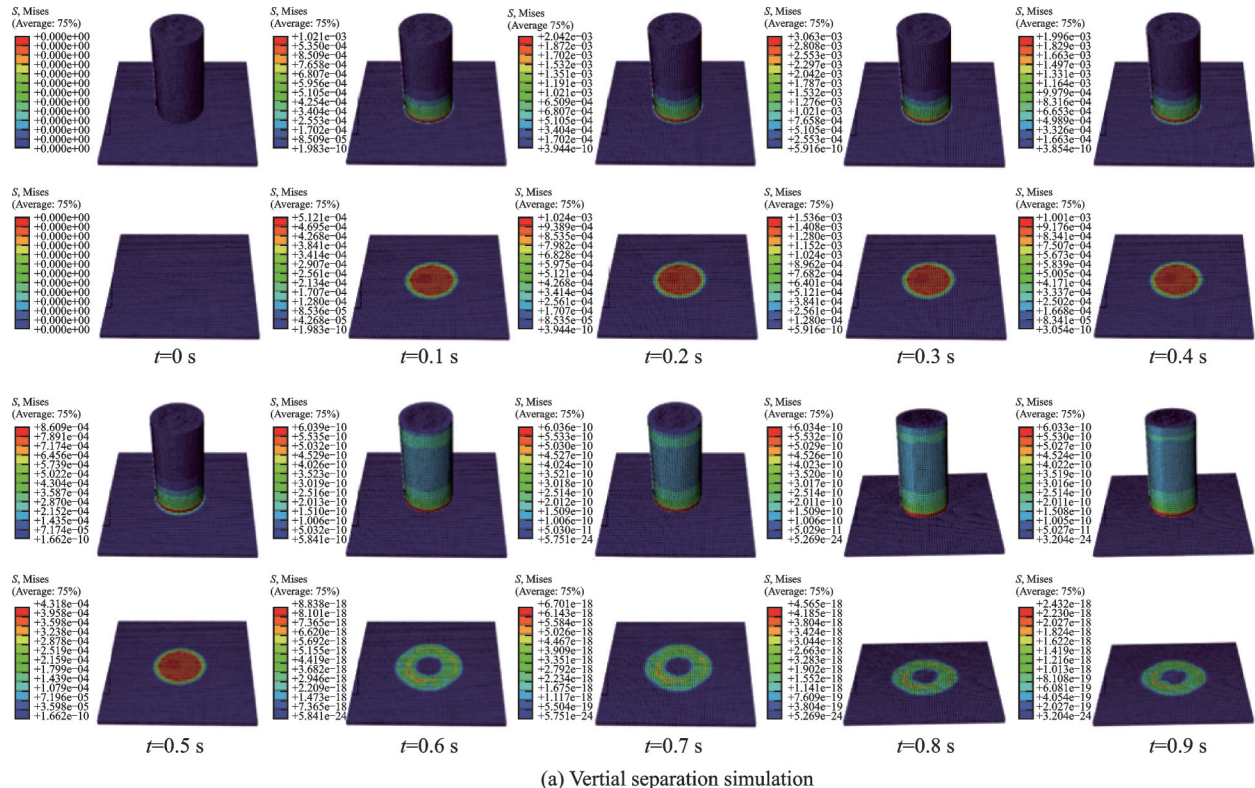
Fig.7 Result comparison

displacement of the ice column, the stress increases gradually until the ice column and the iron sheet fracture. Subsequently, the stress gradually decreases and eventually dissipates. Additionally, it can be observed that the stress distribution varies depending on the direction of the ice column movement. However, the total stress remains consistent throughout the process.

4 Conclusions

The main conclusions of this paper are as follows:

- (1) A test rig was constructed to measure the adhesion between icing icicles and metal planes in both the normal and tangential directions. The study investigated the variation of the normal adhesion



(a) Vertical separation simulation

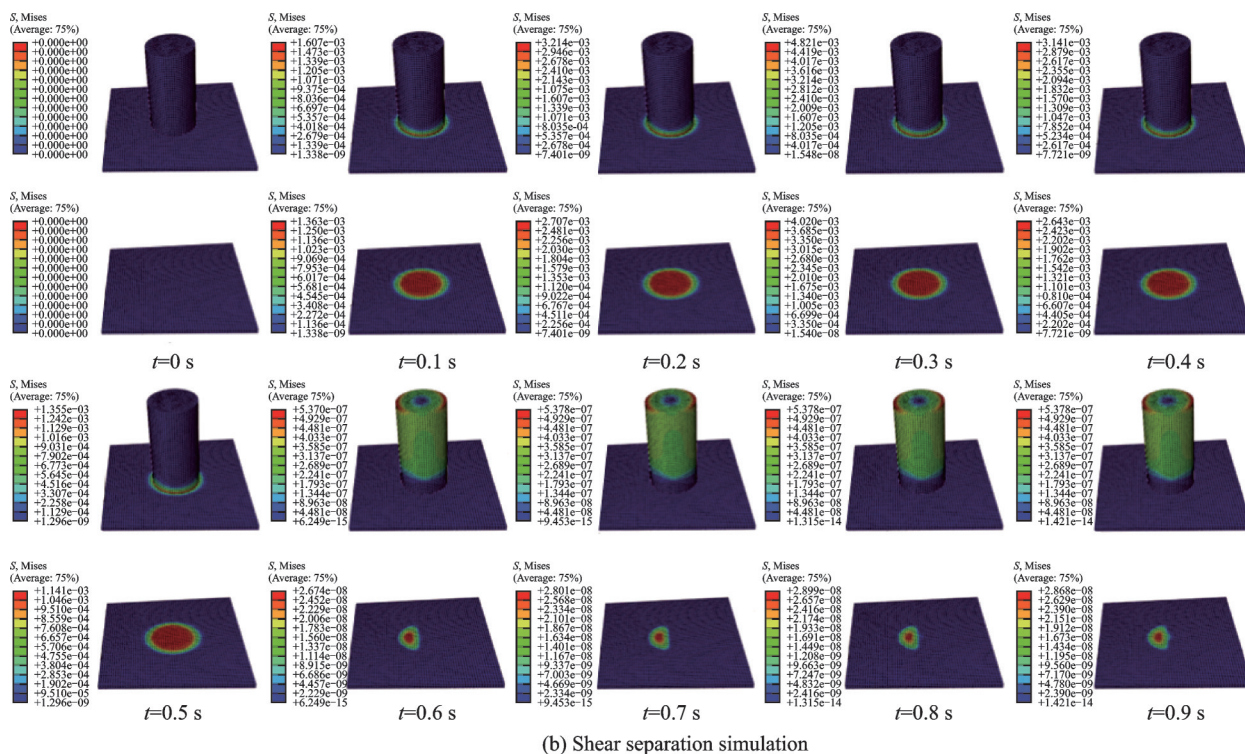


Fig.8 Stress variation cloud diagram during the separation process

and the tangential adhesion at different temperatures. It was observed that as the temperature decreased, both the normal adhesion and the tangential adhesion increased. Additionally, under the same working conditions, the values of the tangential adhesion and the normal adhesion were similar, with the tangential adhesion slightly exceeding the normal adhesion.

(2) The macroscopic icing adhesion model is implemented by incorporating the adhesive unit layer constitutive model. This makes it possible to numerically simulate the separation process between icing and metal walls in a macroscopic form. The icing bonding characteristic data required for the simulation are obtained by experimental means. The separation process of icing and metal sheets is then simulated using Abaqus software.

References

- [1] REEHORST A L, ADDY H E, COLANTONIO R O. Examination of icing induced loss of control and its mitigations: AIAA—2010-8140[R]. [S.I.]: AIAA, 2010.
- [2] LI Hongkun, CHEN Fangfang, GAO Xin. An overview of the research situation on the covering ice of overhead lines[J]. *Electrical Engineering*, 2017(10): 13-15. (in Chinese)
- [3] International Electrotechnical Commission. Wind energy generation systems. Part 1: Design requirements: IEC Switzerland 61400-1 Edition 4[S]. [S.I.]: IEC, 2019.
- [4] LIU S N. The method of handling the icing of ships[J]. *Journal of Northwestern Polytechnical University*, 2007(4): 79-87.
- [5] ZHU Y, PALACIOS J L, ROSE J L, et al. Numerical simulation and experimental validation of tailored wave guides for ultrasonic de-icing on aluminum plates: AIAA—2010-3043[R]. [S.I.]: AIAA, 2010.
- [6] JUNG J M, LEE D H, CHO Y I. Non-newtonian standard viscosity fluids[J]. *International Communications in Heat & Mass Transfer*, 2013, 49: 1-4.
- [7] YANG S, XIA Q, ZHU L, et al. Research on the ice-phobic properties of fluoropolymer-based materials[J]. *Applied Surface Science*, 2011, 257: 4956-4962.
- [8] GE L, DING G, WANG H, et al. Anti-icing property of superhydrophobic octadecyltrichlorosilane film and its ice adhesion strength[J]. *Journal of Nanomaterials*, 2013(10): 1-5.
- [9] KULINICH S, FARZANEH M. On ice-releasing properties of rough hydrophobic coatings[J]. *Cold Regions Science and Technology*, 2011(65): 60-64.
- [10] RONNEBERG S, XIAO S B, HE J Y, et al. Nanoscale correlations of ice adhesion strength and water

contact angle[J]. *Coatings*, 2020, 10(4): 379.

- [11] MI Y, CRISFIELD M A, DAVIES G A O, et al. Progressive delamination using interface element[J]. *Journal of Composite Materials*, 1998, 32(4): 1246-1272.
- [12] BENZEGGAGH M L, KENANE M. Measurement of mixed-mode delamination fracture toughness of uni-directional glass/epoxy composites with mixed-mode bending apparatus[J]. *Composites Science and Technology*, 1996, 56(4): 439-449.

Acknowledgements This work was supported in part by Key Laboratory of Icing and Anti/De-icing of CARDC (No. IADL20210414), the Science and Technology Project of Hebei Education Department (No. JQN2021016). The authors realize that the time and space available for a review of such an ambitious subject are limited and, thus, regretfully,

we are unable to cover many important contributions.

Author Dr. WANG Shaolong received his Ph.D. degree from Northeast Agricultural University in 2017 and has been working in the School of Metallurgy and Energy, North China University of Science and Technology since 2017. His main research direction is icing mechanism and anti-icing equipment development.

Author contributions Dr. WANG Shaolong designed the study, compiled the models, conducted the analysis, interpreted the results and wrote the manuscript. Mr. JI Yanzhuo completed the simulation work of the paper. Mr. KANG Yuhao completed the experimental work of the paper. Prof. SHI Lei and Prof. ZHANG Liang contributed to the discussion and background of the study. All authors commented on the manuscript draft and approved the submission.

Competing interests The authors declare no competing interests.

(Production Editor: XU Chengting)

结冰与金属表面分离过程的数值模拟与实验研究

王绍龙^{1,2,4}, 冀艳卓^{3,4}, 康育浩^{3,4}, 石磊^{3,4}, 张亮^{3,4}

(1. 华北理工大学冶金与能源学院, 唐山 063210, 中国; 2. 中国空气动力研究与发展中心结冰与防除冰重点实验室, 绵阳 621000, 中国; 3. 河北科技师范学院机电工程学院, 秦皇岛 066000, 中国; 4. 河北科技师范学院河北光伏组件制造装备技术创新中心, 秦皇岛 066000, 中国)

摘要:通过研究结冰与物体表面粘结特性,掌握它们之间的分离过程对优化除冰方案具有重要意义。当前研究较多的开展了基于纳米尺度的结冰分离,但其研究内容与真实宏观状态结冰分离过程相差较远,有必要研究宏观尺度的结冰分离过程。本文设计并搭建了用于测试法向和切向结冰粘结力的试验台,在不同温度下展开实验并获得了结冰冰柱与金属表面的法向和切向粘结力。引入宏观的结冰分离机制,引入粘结单元层本构模型,在Abaqus中空对结冰与金属表面分离过程进行数值模拟。通过对比数值模拟和实验验证结果,深入的了解了结冰粘结特性并实现了结冰与金属平面分离过程数值模拟。

Key关键词:冰;粘结力;分离过程;金属表面;数值模拟